The Design of Halbach Arrays for Inductrack Maglev Systems

No.
Richard F. Post
Lawrence Livermore National Laboratory, P.O. Box 808, L-644, Livermore, CA 94551, USA
post3@llnl.gov

Long Nguyen
General Atomics, P.O. Box 85608, MS 86, San Diego, CA 92186-5608, USA
long.nguyen@gat.com

ABSTRACT: The development of the Inductrack maglev system[1] for urban transportation is being pursued at General Atomics in San Diego, California. Central to this development is the optimization of the configuration of permanent magnets of that system, a configuration based on concepts pioneered by the late Klaus Halbach of the Lawrence Berkeley Laboratory. The tools used in this optimization are the computer codes developed at LLNL and GA. These codes have been benchmarked by experiments carried out with the large test wheel at GA, or by a linear-track test facility at LLNL. This paper will discuss the techniques used in performing the optimizations and the issues involved.

.

1 INTRODUCTION

The tools used in these studies are computer codes that were independently developed at LLNL and General Atomics. The results of the computations by these codes were cross-checked against each other with good agreement. In the course of the work several performance-related issues were addressed. These included issues such as the stiffness of the levitation system, the role of higher-order harmonics in the levitating fields, and the effects of the Halbach arrays of the LSM (Linear Synchronous Motor) propulsion system on the system stiffness.

The General Atomics code was originated by Robert Kratz of GA. Most of the calculations were implemented in Mathcad. The code first employs the current sheet model to calculate the magnetic field generated by the permanent magnet Halbach arrays. It then solves the coupled circuit equations of the ladder track guideway, which include the induced voltage generated by the traveling Halbach arrays. Using the calculated induced currents in the track, Lorentz force calculations are then performed to obtain the lift and drag forces. Equations for calculating fields from permanent magnets using a current-sheet model are from the publication "MHD and Fusion Magnets" by R.J. Thome. The inductances used in the coupled circuit equations are obtained from Grover's "Inductance calculations" and the "FastHenry Code".

The two LLNL codes include a modified 2-D code that employs Halbach's theoretical analyses (Halbach, 1980) to determine the magnetic fields from the moving Halbach arrays. The electric field generated by these fields is then used to calculate the currents and the forces in either a ladder-type track or a laminated track. For the track inductance parameters a theoretical value derived by Dmitri Ryutov is used. His expression is based on surface currents induced by the moving fields, taking into account both self- and mutual-inductance terms. In the proper limits Ryutov's expression for the levitation forces reduces exactly to the result derived from first principles.

The LLNL 3-D Halbach array code is based on an Amperian Current formulation. The code has been benchmarked against Halbach's theoretical expressions in the proper limits, showing agreement to three or four significant figures.

2 OPTIMIZATIONS OF THE MAGNETICS

2.1 The Baseline Levitation System

The baseline system for our optimization studies is the one in use in the presently configured test vehicle. The levitation magnet arrays consist of "5 x 3" Inductrack II (Post, 2003) dual Halbach arrays in which the upper array consists of a five-blocks-wide assembly of NdFeB magnets the dimensions of which are 50 mm height, 50 mm transverse width, and 50 mm length . The lower array, three blocks in width, has the same transverse and longitudinal dimensions as those of the upper blocks, but is only 40 mm in height. Figure 1 is a schematic drawing of a cross-section of the baseline system.

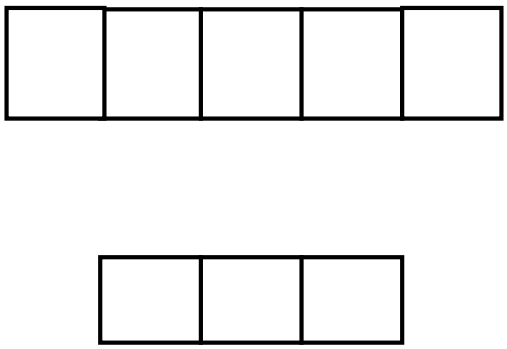

Figure 1: Schematic representation of "5 x 3" baseline Halbach array system.

The arrays are assembled within stainless-steel cans that are mounted transverse to the direction of motion of the car. As a result each row of magnet blocks is separated by a gap of 4 mm. The array configuration number, M = 8, requires that the polarization of the magnets varies by 45° from one row of magnets to the next. The use of an M = 8 configuration, while it leads to higher and more harmonic-free magnetic fields than the M = 4 configuration (90° polarization rotation per row of blocks) is much more expensive to procure than the M = 4 configuration, owing to the need for half of the blocks be polarized at a 45° angle with respect to their faces.

In addition to the levitation force exerted by the 5 x 3 arrays an upward force is exerted by the attractive force between the twin rows of Halbach arrays that comprise the magnets of the LSM drive system and the iron rails above them that provide lateral centering forces. However this attractive force has a negative stiffness (attractive force increasing with decreasing gap) that acts to reduce the positive stiffness associated with the baseline 5 x 3 arrays. In Figure 2 there is plotted the results of an experimental measurement of the force between the LSM magnets and the iron rails, together with an analytic fit to the measurements. The numbers shown are those that would apply for a complete two-chassis train car.

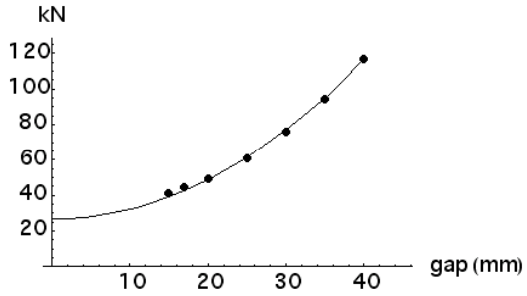

Figure 2: Plot of force exerted by the LSM magnets as a function of the gap between the levitation magnets and the track. Shown also is an analytic fit to the measured forces.

Combining the above-shown force with that calculated for the baseline 5 x 3 configuration there result plots of the change of gap with speed and levitation load and a plot of the total stiffness as a function of levitation gap, as calculated for a velocity of 15 m/sec, and a 500 mm-wide Litz track, i.e. the same track as that used in the present test-track. Figure 3 shows plots of the gap as a function of velocity for levitation loads of 180, 200, 220 and 240 kN. Note the predicted onset of levitation instability at the lowest loads and low speeds.

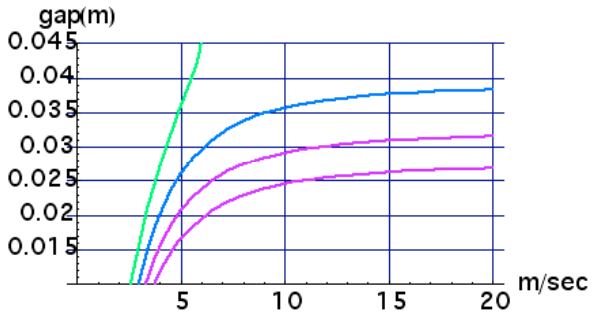

Figure 3: Plots of the gap as a function of velocity for loads of 240 KN (lowest curve), 220 kN, 200 kN, and 180 kN.

The effect of the LSM magnets, being a function of gap and velocity, leads to an increased change in gap with load, even to the point of instability at very light loads as shown in Figure 3.

The above results were calculated with the LLNL 2-D levitation code (as corrected of the gaps between the magnet rows,). Using the same code the net stiffness of the combined 5 x 3 and LSM system was also calculated, with the results shown in Figure 4.

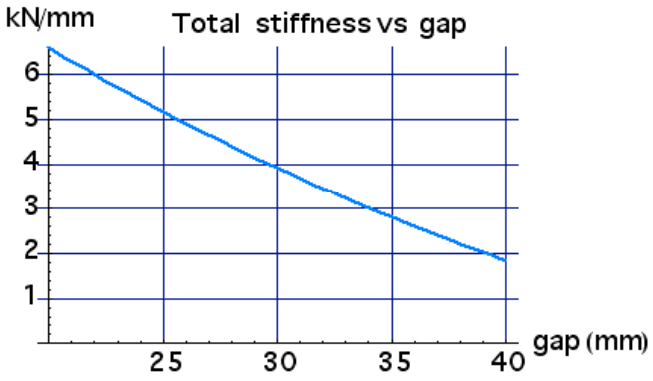

Figure 4: Plot of total stiffness of 5 x 3 plus LSM system vs. levitation gap for velocity of 15 m/sec.

2.2 Levitation System Optimization Goals

The goals of our magnetics optimizations include the following:

(1) Increasing the stiffness of the Inducctrack II primary levitation system.

(2) Reducing the cost of the system , for example by the elimination of the need for magnet blocks with 45° polarization angles. (Requires the use of an M = 4 magnet configuration).

(3) Adopting a geometrical arrangement that permits mounting both the levitation magnets and the LSM magnets in a common housing without mechanical interference between the two sets of magnets.

At the conclusion of the optimization studies we were able to meet all three objectives. Comparison plots of the parameters shown in Figures 4 for the baseline 5 x 3 system will be presented below. A discussion of the final geometry of the optimized magnet configuration will be given in a future report, after experimental data on the performance of the levitation and propulsion system has been obtained.

Figure 5, a plot of the variation of gap with velocity and levitation load, is to be compared with Figure 3, which gives the same data for the baseline case. Note the marked decrease in the spread of the gap as a function of load, together with the absence of any unstable behavior at light loads.

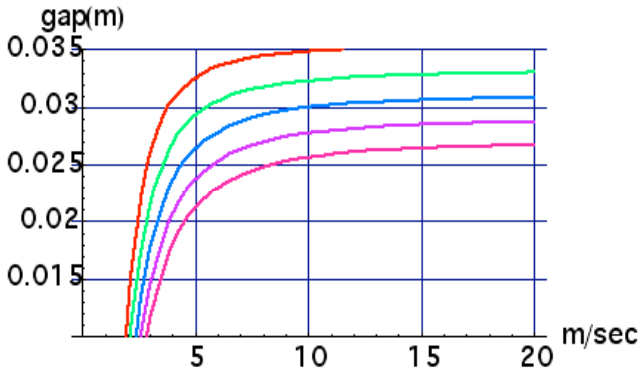

Figure 5: Plots of the gap as a function of velocity for loads of 240 KN (lowest curve), 220 kN, 200 kN, and 180 kN.

Reflecting the reduction in gap variation with load seen in Figure 5, Figure 6 shows the increased stiffness of the optimized configuration relative to that of the baseline 5 x 3 configuration as shown in Figure 4.

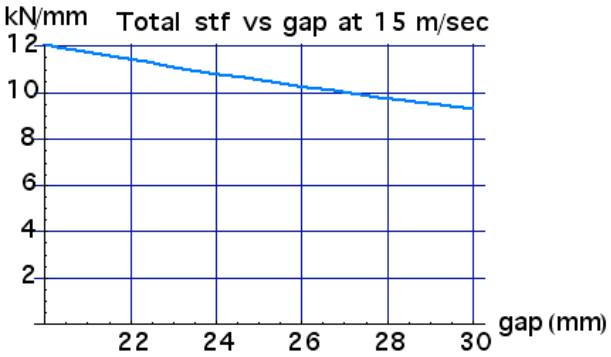

Figure 6: Plot of total stiffness of optimized levitation magnets plus LSM system vs. levitation gap for a velocity of 15 m/sec.

As to the goal No. 2 of the list, reduction in cost of the levitation magnets, quotes from suppliers for the new arrays have been as low a one-half the cost of the baseline levitations arrays. The new

configuration also successfully addresses the geometric constraints described in goal No. 3.

3 RESULTS FROM THE LLNL 3-D CODE

In the LLNL optimization studies the 3-D code was used to benchmark the 2-D code, including correcting the 2-D code for the effect of the gaps between the rows of magnets coming from their encapsulation in stainless steel cans. It was also used to analyze the harmonic content of the waveforms of the M = 4 arrays as employed in the optimized levitation arrays.

With respect to the corrections associated with the gaps between adjacent magnet rows, it was found that the ratio of the integral of the B_x field across the array (including the region of fringing field) associated with a 4 mm gap between blocks 50 mm in width was closely equal to the ratio of the volume of a block divided by the volume represented by the block plus the gap. The 3-D code-computed integral ratio is equal to 0.913, while the volume ratio is equal to 0.926. This result implies that correcting the remanent magnetic field in the 2-D code by a factor equal to the volume ratio as defined above compensates very closely for the effect of a small gap.

The 3-D code was also used to assess the harmonic content of the waveforms of the magnetic fields produced by the M = 4 optimized Halbach array configuration. As predicted by theory (Post and Ryutov, 1996) the only significant harmonic beyond the fundamental is the fifth harmonic, and it decays with distance from the array at five times the rate of decay of the fundamental. Using the 3-D code the waveforms for the magnetic field of a representative M = 4 Halbach array was computed as a function of distance from the face of the array. These waveforms were then analyzed to determine the relative amplitude of the fifth harmonic. Figure 7 is a plot of the computed waveform for the z component of the field, as measured at a gap of 25 mm from the face of the array.

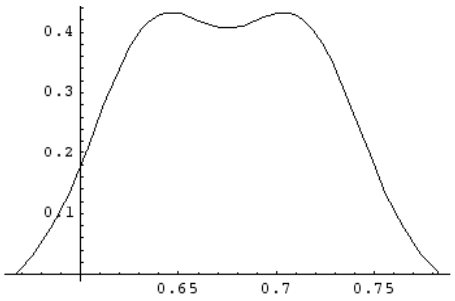

Figure 7: Calculated waveform of B_z for M = 4 Halbach array with wavelength of 0.432 m. and at a gap of 25 mm.

These data were fitted by an exponential function representing the theoretically predicted ratio of the fifth, with the fitting curve normalized at one of the data points. Figure 8 is a plot of the data shown together with that of the fitting function.

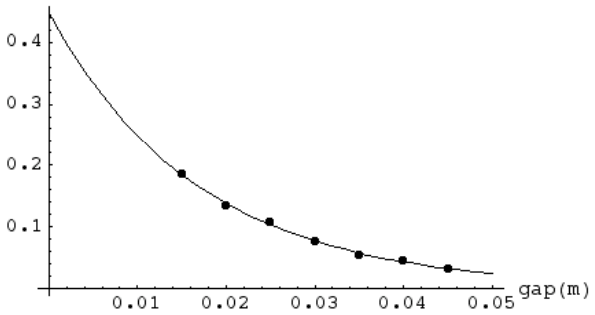

Figure 8: Plot of the ratio of the fifth harmonic of the M = 4 magnetic field vs. gap, shown together with the theoretically predicted decay curve.

As can be seen from the plot in Figure 8, the amplitude of the fifth harmonic at typical levitation gaps (e.g. 25 mm) is of order 10 percent of that of the fundamental. Since we are here dealing with a set of orthogonal functions no cross-product terms will appear in the analysis of the levitation caused by each harmonic. Since this contribution varies as the square of the amplitude of the harmonic it is clear that the contribution of the fifth harmonic (of order 0.1 squared) is very small compared to that of the fundamental and can safely be neglected in computing the levitation force.

4 RESULTS FROM GA CODE

The results discussed above for the baseline levitation system and the optimized levitation arrays were independently confirmed by GA code.

4.1 Baseline Levitation System

The calculated lift forces for the baseline 5 x 3 Halbach array using GA code are plotted in Figure 9 as a function of velocity for various levitation gaps. At a nominal gap of 25 mm and a speed of 15 m/sec the baseline array can provide about 170 kN lift force. The force stiffness about this operating point is 8 kN/mm. The total stiffness when included the LSM attractive force (discussed in Section 2) is less than 6 kN/m.

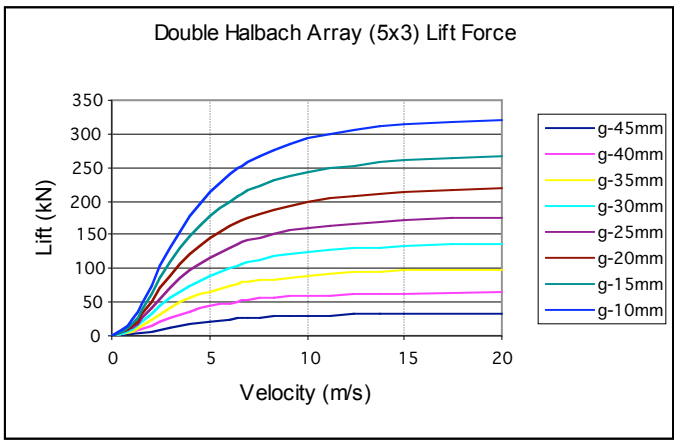

Figure 9: Lift force of the 5 x 3 baseline array as a function of velocity for various levitation gaps.

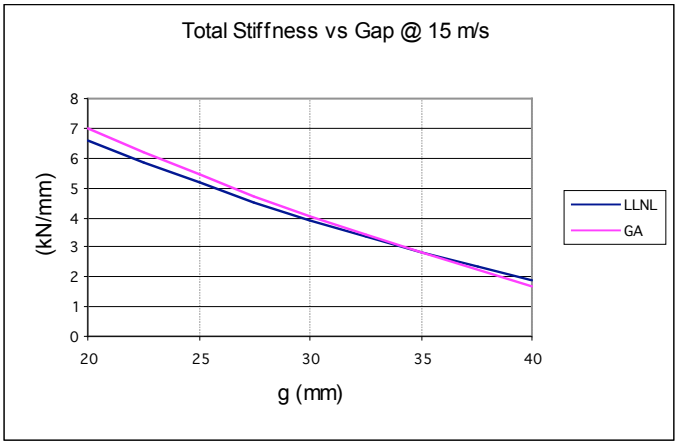

Figure 10: Total stiffness of 5 x 3 array plus LSM system vs. levitation gap for velocity of 15 m/sec.

The total stiffness when combined both the 5 x 3 baseline array lift force and the LSM attractive force for a velocity of 15 m/sec is plotted as function of levitation gap in Figure 10. The LLNL result shown in Figure 4 is also re-plotted in the same figure for comparison. Good agreement can be seen from the two codes. There is about 5 percent different between the two codes at a levitation gap of 25 mm.

4.2 Optimized Levitation Array

The calculated lift forces for the optimized levitation array (discussed in Section 2.2) using the GA code are plotted in Figure 11 as a function of velocity for levitation gap varying from 10 mm to 50 mm. It can be observed that the lift force of the optimized array has much wider changes with respect to the changes in the gap. This indicates that the optimized array is much more stiff than the baseline array. At a nominal gap of 25 mm and a speed of 15 m/s, the optimized array can generate a lift force of 175 kN (slightly higher than the baseline array). And the stiffness about this point is almost 13 kN/mm, which is much higher than that of the baseline array.

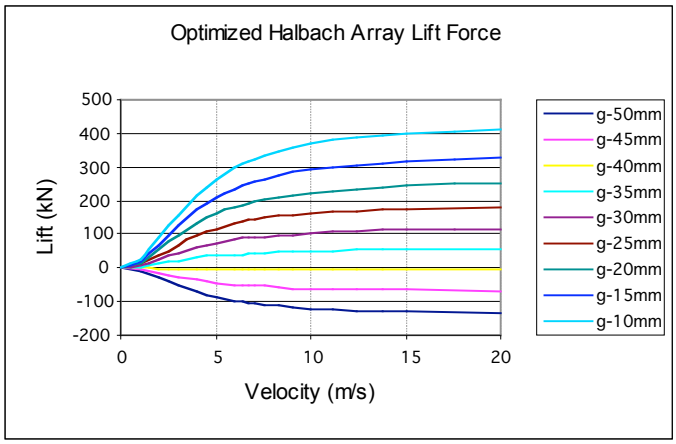

Figure 11: Lift force of the optimized Halbach array as function of velocity for levitation gap varying from 10 mm to 50 mm.

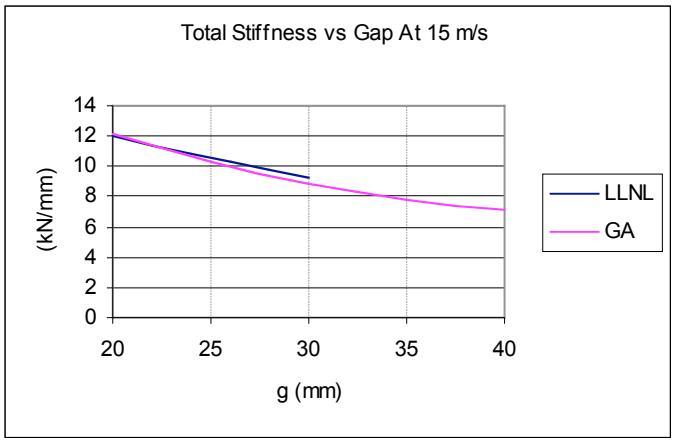

Figure 12: Total stiffness of optimized levitation array plus LSM system vs. levitation gap for velocity of 15 m/sec.

The total stiffness of the optimized levitation array plus the LSM system at 15 m/sec is plotted as a function of levitation gap in Figure 12. Also plotted in the same figure is the result from LLNL code.

Again, good agreement can be observed from the two codes. The difference between the two codes is within 5 percent out to 30 mm gap. The result from GA code confirmed the increase in stiffness of the optimized configuration relative to that of the baseline 5 x 3 configuration.

5 SUMMARY

An important element of the ongoing program at General Atomics aimed at the commercialization of maglev systems based on the Inductrack concept has been the optimization of the Halbach-array magnet system itself. Starting from the baseline "5 x 3" magnet array employed in the full-scale test track at General Atomics several different "optimized" magnet configurations were studied, using computational tools developed independently at the Lawrence Livermore National Laboratory and at General Atomics. Among the goals of the optimization were: to increase the stiffness of the levitation forces, to reduce the cost of manufacturing and encapsulating the arrays, and to improve the geometry of the levitation arrays vis á vis the magnets of the LSM, The later are to be housed in the same stainless-steel "cans" that contain the rows of Halbach-array levitation magnets. In the optimization studies performed at the Lawrence Livermore National Laboratory all three of these objectives were addressed, using the codes developed at the Laboratory. The proposed configurations were then independently analyzed at General Atomics, using their computer codes. Close agreement between the results was found for all of the critical parameters. Based on these confirming results the magnets were ordered from a supplier. and the modified arrays are to be installed in the two new test-track chasses now being constructed.

The work of one of the authors (RFP) was performed under the auspices of the U.S. Department of Energy by Lawrence Livermore National Laboratory under Contract DE-AC52-07NA27344.

5 REFERENCES

Halbach, J. K. (1980) "Design of Permanent Multipole Magnets with Oriented Rare Earth Cobalt Material", *Nuclear Instruments and Methods*, vol. 169, no. 1, 1980, pp. 1-10.

Grover, F. W. (1946) "Inductances Calculations: Working Formulas and Tables", New York, Dover.

Post, R. F. and Ryutov, D. D. (1996) LLNL Report No. UCRL-30-124115, "The Inductrack Concept: a New Approach to Magnetic Levitation."

Post, R. F. (2003) U.S. Patent No. 6,633,237 B2, "Inductrack Magnet Configurations."

Thome, R. J. and Tarrh, J. M. (1982) "MHD and Fusion Magnets: Field and Forces Design Concepts", New York, John Wiley & Sons.